CHEMISTRY
A EUROPEAN JOURNAL

FULL PAPER

DOI: 10.1002/chem.201300203

Intramolecular [2+2] Photocycloaddition of 3- and 4-(But-3-enyl)oxyquinolones: Influence of the Alkene Substitution Pattern, Photophysical Studies, and Enantioselective Catalysis by a Chiral Sensitizer

Mark M. Maturi,[a] Matthias Wenninger,[b] Rafael Alonso,[a] Andreas Bauer,[a] Alexander Pöthig,[a] Eberhard Riedle,*[b] and Thorsten Bach*[a]

Abstract: The intramolecular [2+2] photocycloaddition of four 4-(but-3-enyl)oxyquinolones (substitution pattern at the terminal alkene carbon atom: CH_2, *Z*-CHEt, *E*-CHEt, CMe_2) and two 3-(but-3-enyl)oxyquinolones (substitution pattern: CH_2, CMe_2) was studied. Upon direct irradiation at $\lambda = 300$ nm, the respective cyclobutane products were formed in high yields (83–95%) and for symmetrically substituted substrates with complete diastereoselectivity. Substrates with a *Z*- or *E*-substituted terminal double bond showed a stereoconvergent reaction course leading to mixtures of regio- and diastereomers with almost identical composition. The mechanistic course of the photocycloaddition was elucidated by transient absorption spectroscopy. A triplet intermediate was detected for the title compounds, which–in contrast to simple alkoxyquinolones such as 3-butyloxyquinolone and 4-methoxyquinolone–decayed rapidly ($\tau \approx 1$ ns) through cyclization to a triplet 1,4-diradical. The diradical can evolve through two reaction channels, one leading to the photoproduct and the other leading back to the starting material. When the photocycloaddition was performed in the presence of a chiral sensitizer (10 mol%) upon irradiation at $\lambda = 366$ nm in trifluorotoluene as the solvent, moderate to high enantioselectivities were achieved. The two 3-(but-3-enyl)oxyquinolones gave enantiomeric excesses (*ee*s) of 60 and 64% at −25 °C, presumably because a significant racemic background reaction occurred. The 4-substituted quinolones showed higher enantioselectivities (92–96% *ee* at −25 °C) and, for the terminally *Z*- and *E*-substituted substrates, an improved regio- and diastereoselectivity.

Keywords: cycloaddition · enantioselectivity · photochemistry · sensitizers · time-resolved spectroscopy

Introduction

Quinolone [2+2] photocycloaddition reactions[1] are known since the late 1960s when Evanega and Fabiny reported on the intermolecular reaction of the parent compound (carbostyril) with various alkenes.[2] These studies were preceded by work of Taylor et al.,[3a] Elliott,[3b] and Buchardt[3c] on the [2+2] photodimerization of quinolones. The initial report by Evanega and Fabiny[2a] was followed in rapid succession by several significant contributions from other research groups, most notably from the group of Naito and Kaneko in the 1980s.[4] Intramolecular [2+2] photocycloaddition reactions were first reported in 1979[4f] and a few reactions of this type were subsequently studied more closely.[4g,s,5] The synthetic importance of quinolone [2+2] photocycloaddition is mainly due to further ring-opening reactions at the cyclobutane ring,[1a,e,6] which enable access to highly substituted quinolone derivatives (see below).

Mechanistic work on the quinolone [2+2] photodimerization and [2+2] photocycloaddition has revealed that the reactions proceed through the respective triplet excited state (T_1), which is populated by direct excitation at $\lambda = 300$–350 nm to the first excited singlet state (S_1) and subsequent rapid intersystem crossing.[4d,7] The triplet state can also be populated by sensitization employing compounds with high triplet energy states, for example, benzophenone. The triplet state energy of the parent quinolone has been reported as $E(T_1) = 276$ kJ mol^{-1} corresponding to the energy of a 434 nm photon.[7a] The photodimerization of quinolones has been studied by laser flash photolysis,[7a,b,8] however, to the best of our knowledge, the course of the intramolecular [2+2] photocycloaddition of quinolones has until recently

[a] M. M. Maturi,[+] Dr. R. Alonso,[+] Dr. A. Bauer, Dr. A. Pöthig, Prof. Dr. T. Bach
Department Chemie and
Catalysis Research Center (CRC)
Technische Universität München
Lichtenbergstrasse 4
85747 Garching (Germany)
Fax: (+49) 89-289-13315
E-mail: thorsten.bach@ch.tum.de

[b] M. Wenninger,[+] Prof. Dr. E. Riedle
Lehrstuhl für BioMolekulare Optik
Ludwig-Maximilians-Universität
Oettingenstrasse 67, 80538 München (Germany)
E-mail: riedle@physik.uni-muenchen.de

[+] These authors contributed equally to this work.

Supporting information for this article is available on the WWW under http://dx.doi.org/10.1002/chem.201300203.

(see below)[9] not been investigated by transient absorption spectroscopy.

[2+2] Photocycloaddition reactions of quinolones were initially studied in our group[5b,10] in the context of enantioselective photochemical reactions mediated by a chiral template.[11] Two-point hydrogen-bonding of the quinolone lactam to the lactam part of a chiral bicyclic skeleton[12] derived from Kemp's triacid[13] led to an efficient enantioface differentiation. An intermolecular reaction of this type was implemented as key step in the first enantioselective total synthesis of the *Melodinus* alkaloid (+)-meloscine. In this case, a ring expansion of the cyclobutane to a cyclopentanone was achieved by a retro-benzilic acid rearrangement.[14]

When searching for catalytic enantioselective photochemical reactions,[15] we discovered that dextrorotatory xanthone (+)-**1** and its levorotatory enantiomer (−)-**1** exhibit superior catalytic activity in intramolecular quinolone [2+2] photocycloaddition reactions provided that the reacting quinolone was appropriately chosen (Scheme 1).[9,16] It was found that

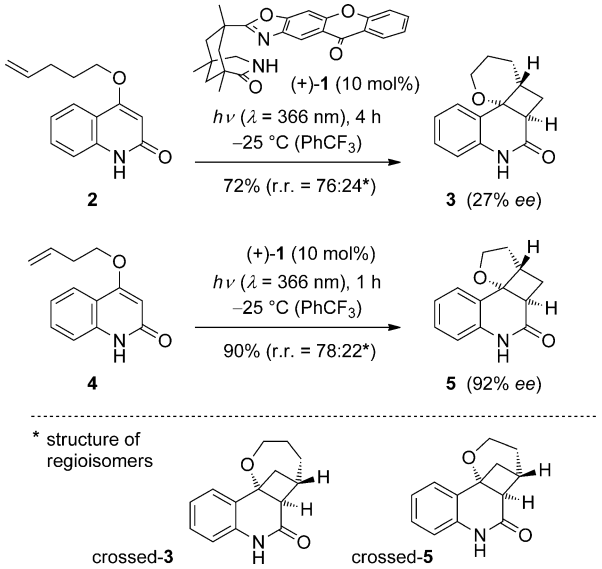

Scheme 1. Major differences in the enantioselectivity (*ee*) of the intramolecular [2+2] photocycloaddition of 4-(pent-4-enyl)oxyquinolone (**2**) and 4-(but-3-enyl)oxyquinolone (**4**) upon sensitization with xanthone (+)-**1**; structure of crossed regioisomers crossed-**3** and crossed-**5** (r.r. = regioisomeric ratio).

the reaction of 4-(but-3-enyl)oxyquinolone (**4**) proceeded under identical conditions with a significantly higher enantioselectivity than the reaction of 4-(pent-4-enyl)oxyquinolone (**2**), the alkyl tether of which is longer by one methylene group than the tether of the former substrate.

The binding properties of both substrates **2** versus **4** and products **3** versus **5** to lactam (+)-**1** should be almost identical. Indeed, it had been previously shown that the reactions **2**→**3** and **4**→**5** proceed with high enantioselectivity in the presence of a stoichiometrically employed template,[9,10c] which bears the same 1,5,7-trimethyl-3-azabicyclo-[3.3.1]nonan-2-one skeleton as catalyst **1**. Consequently, the different behavior in the catalytic reaction seemed to arise from the different kinetic parameters involved in the respective [2+2] photocycloaddition. It was speculated that upon triplet sensitization within a substrate–catalyst complex the subsequent cyclization to an intermediate 1,4-biradical should be faster for substrate **4** (five-membered ring formation) than for substrate **2** (six-membered ring formation). The rate of dissociation from the chiral lactam (+)-**1** competes efficiently with the cyclization rate in the latter case, causing this reaction to occur with lower enantioselectivity. Indeed, it was experimentally shown that the triplet lifetime of compound **4** is significantly shorter than the triplet lifetime of compound **2**. The lifetime of compound **2** in deaerated trifluorotoluene at ambient temperature could be determined by laser flash photolysis as $\tau\,[T_1(\mathbf{2})] = 57$ ns. However, the detection limit of the laser setup did not allow for an accurate determination of $\tau\,[T_1(\mathbf{4})]$, which was estimated to be at least by a factor of 0.4 shorter than $\tau\,[T_1(\mathbf{2})]$.[9]

In the present study we have largely broadened the scope of quinolone substrates and investigated the reaction behavior of differently substituted 3- and 4-(but-3-enyl)oxyquinolones **6**–**9** (Figure 1) in the absence and the presence of a chiral sensitizer.

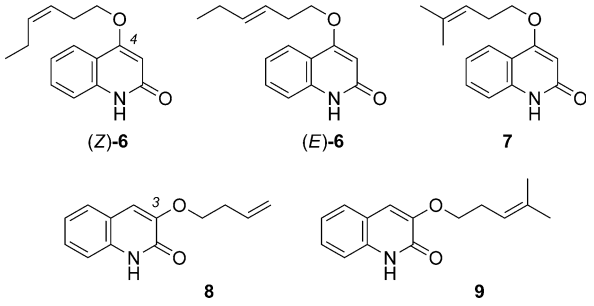

Figure 1. Quinolone substrates **6**–**9** employed in this study.

The key objective of the study was to prove for 4-(but-3-enyl)oxyquinolones that a higher cyclization rate consistently leads to high enantioselectivity. By using the diastereomerically pure substrates (*Z*)-**6** and (*E*)-**6**, conclusions regarding the stereospecificity of the reaction were expected to be drawn. Data for the enantioselective reactions were collected at three different temperatures (−25 °C, 0 °C, and RT). The yet completely unexplored 3-(but-3-enyl)oxyquinolones were studied for comparison. The reaction kinetics of the photocycloaddition was followed by transient absorption spectroscopy both on the fs–ps and on the ns–μs timescale to provide a comprehensive picture of the reaction course through the respective singlet- and triplet state lifetimes.

Results and Discussion

Synthesis of the quinolone substrates: The synthesis of 4-(but-3-enyl)oxyquinolones **6** and **7** (Scheme 2) commenced

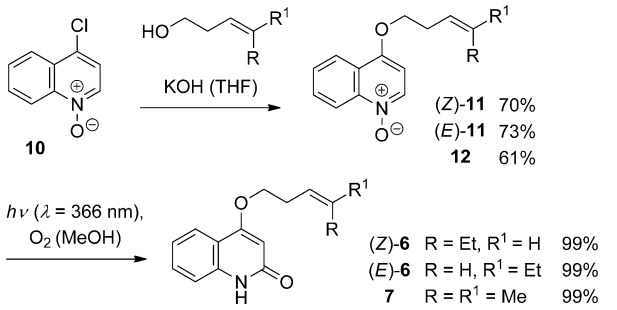

Scheme 2. Synthesis of 4-(alk-3-enyl)oxyquinolones **6** and **7** from 4-chloroquinolin-*N*-oxide (**10**) by nucleophilic substitution and subsequent photochemical rearrangement.

with an aromatic nucleophilic substitution reaction at 4-chloroquinolin-*N*-oxide[17] (**10**). The respective alcohols, which were required to produce the substitution products **11** and **12**, are commercially available. The subsequent rearrangement of the *N*-oxides to the desired products was performed according to a previously reported method,[18] which we have optimized in recent years.[19] Two modifications are crucial. Firstly, the reaction, which proceeds at the singlet hypersurface, is performed in an oxygen-saturated methanol solution, which avoids reactions of the products from the triplet state (see below). Secondly, a continuous flow system is being used for irradiation, which allows one to optimize the exposure time of the substrates to the light source. It was gratifying to note that this optimization has led to a high level of reproducibility and generality. Product formation was essentially quantitative in all cases and side products were not detected (Scheme 2).

The preparation of 3-(but-3-enyl)oxyquinolones **8** and **9** was straightforward based on literature precedence (Scheme 3). Known 3-hydroxyquinolone (**13**)[20] was treated

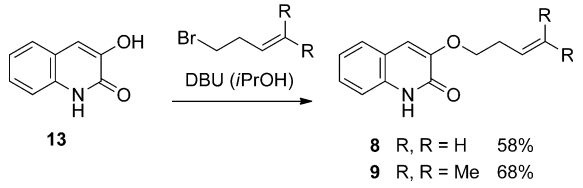

Scheme 3. Synthesis of 3-(alk-3-enyl)oxyquinolones **8** and **9** from the respective bromides by nucleophilic substitution with 3-hydroxyquinolone (**13**).

with the respective alkenyl bromides and 1,8-diazabicyclo-[5.4.0]undec-7-ene (DBU) in isopropanol[21] to deliver the desired products by nucleophilic substitution. In an analogous fashion, 3-butoxyquinolone was prepared from **13** and butyl bromide.

[2+2] Photocycloaddition reactions in the absence of a sensitizer at $\lambda = 300$ nm: To check the general feasibility of the photocycloaddition and to secure racemic material for analytical purposes, reactions were performed at $\lambda = 300$ nm (light source: RPR-3000 Å, emission spectrum, see the Supporting Information; $c = 5$ mM). Since the quinolone absorption is relatively high at this wavelength, [2+2] photocycloaddition reactions tend to proceed smoothly without addition of a sensitizer. Indeed, 4-(hex-3-enyl)oxyquinolones (**6**) were converted within 40 min into the respective products. Surprisingly, the regioselectivity was relatively low and, besides the straight products *rac*-**14**, significant amounts of the crossed product *rac*-**15** were obtained (Scheme 4). The

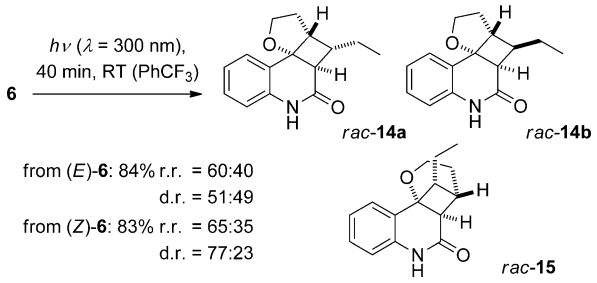

Scheme 4. Intramolecular [2+2] photocycloaddition of 4-(hex-3-enyl)oxyquinolones (**6**) to straight products *rac*-**14** and crossed product *rac*-**15** (r.r. = **14**:**15**; d.r. = **14a**:**14b**); light source: RPR-3000 Å (emission spectrum, see the Supporting Information).

straight products *rac*-**14** were formed as two diastereoisomers with *rac*-**14a** prevailing over *rac*-**14b**. A second crossed diastereoisomer apart from *rac*-**15** was not observed. The relative configuration of the products was proven by extensive one- and two-dimensional ^{1}H NMR studies (see the Supporting Information for further details). Although it is not apparent from the two-dimensional drawings, the preference for the respective diastereoisomer *rac*-**14a** in the straight series and *rac*-**15** in the crossed series can be readily understood from three-dimensional molecular models. In the minor straight diastereoisomer *rac*-**14b**, the ethyl group shows a major steric interaction with the dihydroquinolone ring, which makes the formation of this diastereoisomer less favorable. The situation, that is, the interaction of the ethyl group with the dihydroquinolone ring, would be even worse in the diastereoisomer of *rac*-**15**, which is consequently not formed at all. The photocycloaddition was not stereospecific as expected from a reaction occurring mainly in the triplet manifold.[22,23]

Even the *E* isomer (*E*)-**6**, with the ethyl group and the alkyl chain in a relative *trans*-configuration, gave predominantly products *rac*-**14a** and *rac*-**15**, in which these substituents are *cis*-positioned. The fact that the relative product ratios (regioisomeric ratio (r.r.) and diastereomeric ratio (d.r.)) are not completely identical for (*Z*)-**6** and (*E*)-**6** seems to indicate a minor contribution of the singlet excited state (S_1) to the net reaction. Based on the transient spectroscopy data (see below), however, it is more likely that differences in the first bond formation and in the subsequent reaction branching within the triplet manifold are responsible for this result. The *Z* isomer (*Z*)-**6** exhibits more than a two-fold product efficiency relative to (*E*)-**6**. If the irradiation

experiments were stopped before the conversion was complete, the re-isolated starting material **6** showed epimerization around the double bond. At 0 °C the reactions (c = 5 mM in $PhCF_3$) were interrupted after five minutes of irradiation. If *Z*-**6** was employed as starting material, the conversion was 60 % and the re-isolated substrate showed an *E*/*Z* ratio of 31/69. If *E*-**6** was used, the conversion was 44 % and starting material **6** was recovered in an *E*/*Z* ratio of 51/49.

The outcome of the [2+2] photocycloaddition of substrate **7** was less complex than that of substrates **6**. Indeed, a single reaction product *rac*-**16** was obtained in high yield (Scheme 5). Complete conversion was achieved after 3.5 h (c = 5 mM).

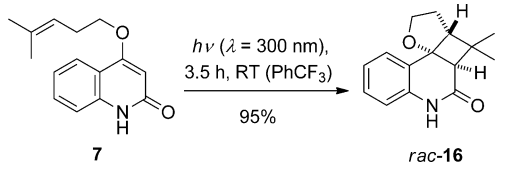

Scheme 5. Selective intramolecular [2+2] photocycloaddition of 4-(4-methylpent-3-enyl)oxyquinolone (**7**) to straight product *rac*-**16**.

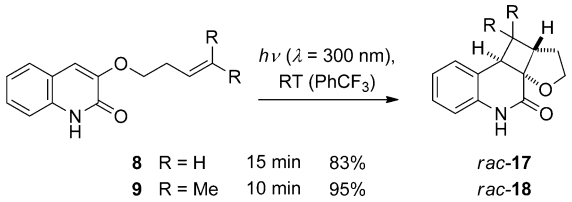

Scheme 6. Selective intramolecular [2+2] photocycloaddition of 3-(alk-3-enyl)oxyquinolones **8** and **9** to straight products *rac*-**17** and *rac*-**18**.

Similarly, the reaction of 3-(alk-3-enyl)oxyquinolones **8** and **9** (c = 2.5 mM) proceeded smoothly providing single products *rac*-**16** and *rac*-**17** in high yields (Scheme 6). It is notable that the crossed regioisomer was not observed in the photocycloaddition of 3-(but-3-enyl)oxyquinolone (**8**). The reaction of the 4-substituted analogue **4** delivers under identical conditions the cycloaddition products in a regioisomeric ratio of 86:14.[9] The regioselective outcome of the reaction of substrate **9** is in accord with the above-mentioned reaction of the 4-substituted analogue **7**. The reaction times required for complete conversion were relatively short for the 3-alkenyloxy-substituted quinolones **8** and **9** reflecting in part their higher absorption at λ = 300 nm (see below).

Transient absorption spectroscopy on multiple timescales: Time-resolved spectroscopic studies, both on the fs–ps and on the ns–µs timescale, were performed with all newly prepared quinolones **6**–**9** as well as with the previously reported substrate **4**. Two major goals were associated with this study. The first goal was to obtain precise data about the liftetimes τ [T_1] of the triplet intermediates derived from substrates **4** and **6**–**9**. Given the previously mentioned assumption of a rapid five-membered ring cyclization it was expected that these lifetimes are significantly shorter than the 57 ns determined for τ [T_1(**2**)].[9] A second goal was to substantiate the mechanistic course of the intramolecular quinolone [2+2] photocycloaddition in an extended time interval (fs–µs) with detection of all relevant intermediates. Time-resolved spectroscopic data covering a sufficient temporal and spectral range for quinolone [2+2] photocycloaddition reaction are scarce[7–9] and it was required to obtain a solid database for future studies.

All decay rates and species-associated spectra (SAS) of the occurring intermediate states discussed below were determined by applying a global data analysis on the measured data matrices (see the Experimental Section). 4-Methoxyquinolone (**19**) and 3-butoxyquinolone (**20**), which cannot react in an intramolecular [2+2] photocycloaddition, served as reference to study the intrinsic photophysical properties such as lifetime and spectral properties of the S_1 and T_1 state (Figure 2).

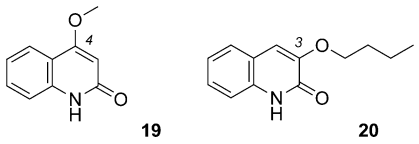

Figure 2. Structures of 4-methoxyquinolone (**19**) and 3-butoxyquinolone (**20**), which were used in the present study as reference compounds.

The excitation wavelength was λ = 270–275 nm in all transient spectroscopy measurements. A reference measurement for **4** at λ = 330 nm showed that the observed dynamics are not changed by the excitation to the S_2 state instead of the S_1 state. Since the influence of pump stray light can be dramatically reduced by the shorter wavelength, this choice was preferred. To secure optical transparency in the UV range and due to solubility reasons, acetonitrile was employed as the solvent in all experiments ensuring a homogeneous solution of equal concentration ($c \approx$ 0.5 mM, optical density [318 nm, 1 mm] $\approx$ 0.5) for all substrates. The studies were performed under aerobic conditions at room temperature. The solubility of oxygen in air-equilibrated acetonitrile is known to be 2.4 mM[24] and at this oxygen concentration an interference with intramolecular reaction processes (displaying rate constants larger than 10^7 s^{-1}) was not to be expected.[25]

For the time-resolved measurements and their interpretation the steady-state absorption and emission spectra of all compounds were determined. As expected, the spectral properties were equal within the measurement error for all 4-substituted quinolones (**19**, **4**, (*Z*)-**6**, (*E*)-**6**, **7**) and for all 3-substituted quinolones (**20**, **8**, **9**), since the electronic properties of the absorbing chromophore remain constant within each substrate series. The measured spectra are exemplarily shown for both chromophores **19** and **20** in Figure 3. Although the shape of the spectra is very similar for the two compounds, it should be noted that the absorption of the 3-

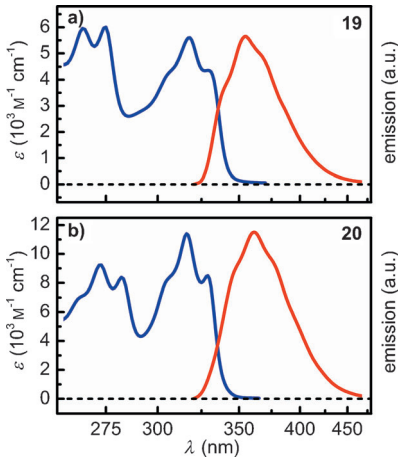

Figure 3. UV/Vis absorption spectra ($c \approx 0.1$ mM) and normalized emission ($c \approx 0.01$ mM) after 315 nm excitation of a) 4-methoxyquinolone (**19**) and b) 3-butoxyquinolone (**20**) in MeCN, which are typical for all other studied quinolones.

substituted quinolone, that is, compound **20**, is by a factor 2 more intense than the absorption of **19**. The steady-state spectra allow estimating the radiative decay rate k_{rad} of the S_1 state according to Strickler and Berg.[26] We calculated the values of $k_{rad} = (14\ ns)^{-1}$ for **19** and $k_{rad} = (9\ ns)^{-1}$ for **20**.

The photophysical properties of reference compounds **19** and **20** were studied by transient absorption spectroscopy. A very broad, weakly structured excited state absorption of the S_1 state was found, which is overlaid by signals of ground state bleach (310–340 nm) and stimulated emission (370–450 nm) both for **19** (compare $\Delta t = 1$ ps in Figure 4a) and **20**. The lifetime of the S_1 state is dominated by a relatively fast intersystem crossing (ISC) into the triplet manifold on the 250 ps timescale. Exact values for the S_1 lifetime of the various compounds are given in Table 1. Since the competing radiative deactivation of the S_1 state occurs on

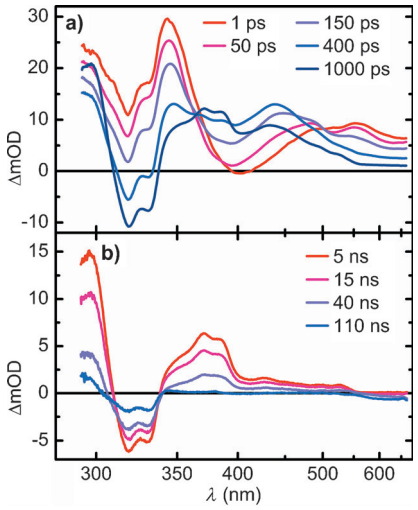

Figure 4. Transient absorption from measurements on the ps (a) and on the ns (b) timescale of quinolone **4** in MeCN at selected pump-probe delays Δt after 270 nm excitation.

Table 1. Parametrization of the excited state dynamics of all synthesized quinolones: The S_1 lifetime τ [S_1], the triplet lifetime τ [T_1] and the triplet 1,4-diradical lifetime τ [T-DR] were directly obtained from transient absorption spectroscopy. The quantum yield for product formation Φ_P was determined by actinometric measurements. The quantum yields for triplet formation Φ_{T1}, population of the triplet 1,4-diradical Φ_D and the ratio k_{clos}/k_{retro} of the rates for second bond-formation and retrosynthetic disconnection were calculated on the basis of a sequential rate model.[a]

Entry		τ (S_1) [ps]	τ (T_1) [ns]	τ (T-DR) [ns]	Φ_P	Φ_{T1}	Φ_D	k_{clos}/k_{retro}
1	**19**	229	116	–	–	0.98	–	–
2	**4**	237	0.651	29	0.30	0.98	0.98	31:69
3	(*Z*)-**6**	199	1.319	30	0.72	0.99	0.97	74:26
4	(*E*)-**6**	202	0.934	32	0.32	0.99	0.98	33:67
5	**7**	176	0.647	34	0.26	0.99	0.98	26:74
6	**20**	296	81	–	–	0.97	–	–
7	**8**	362	≈1.5[b]	23	0.73	0.96	0.95	77:23
8	**9**	301	0.957	25	0.54	0.97	0.96	57:43

[a] The excitation wavelength was $\lambda = 270$–275 nm in all transient spectroscopy measurements. Acetonitrile was employed as the solvent ensuring a homogeneous solution of equal concentration ($c \approx 0.5$ mM, optical density [318 nm, 1 mm] ≈ 0.5) for all substrates. [b] The lifetime is in a time window that is not well-covered with the fs–ps (too slow) or with the ns–μs (too fast) setup.

the 10 ns timescale (see above), a triplet yield close to unity can be assumed (see Table 1). A direct return to the electronic ground state by internal conversion can be excluded due to the lack of any significant ground state bleach component in the spectrum associated with the 250 ps decay (see the Supporting Information). The lowest triplet state exhibits a clear absorption band centered at 450 (**19**) and 400 nm (**20**), respectively, which is in agreement with reported triplet spectra of related compounds.[7a,b] According to previous data,[9] the triplet state lifetime of **19** in degassed trifluorotoluene is in the μs range. Due to oxygen-mediated triplet quenching we observe a significantly reduced lifetime in the 100 ns domain both for **19** and **20** in air-equilibrated MeCN. The exact values are summarized in Table 1.

Since all synthesized quinolones **4** and **6**–**9**, which can undergo intramolecular [2+2] photocycloaddition, qualitatively show the same photochemical behavior and only differ quantitatively, the following discussion of the reaction kinetics is based on quinolone **4** (Figure 4). Compound **4** exhibits after excitation the same spectral properties of the S_1 state as already observed for the reference compound **19** (see Figure 3a). ISC occurs on the 100 ps timescale, whereas the lifetime τ [T_1] of the triplet state is significantly reduced compared with reference **19**. We find a lifetime of τ [T_1(**4**)] = 651 ps as compared to τ [T_1(**19**)] = 116 ns (Table 1). However, in contrast to **19**, the T_1 state of **4** does not decay to the ground state, but a third state with a significant remaining ground state bleach signature is populated. Since the competing decay of the T_1 state by oxygen-mediated triplet quenching occurs on a much longer timescale (as measured for **19**) a close to unity quantum yield for the population of this newly formed state can be safely assumed. This transient state decays with a time constant of τ [T-DR(**4**)] = 29 ns. The remaining spectral signature is perma-

nent within the observed temporal window of several μs and significantly lower in ground state bleach intensity than its parent state. This observation strongly indicates that the parent state is depopulated by two competing processes: one leading back to the starting material and another one leading to the formation of a stable product, which does not absorb in the spectral range above 300 nm (see Figure 4b).

The transient absorption spectra are fully in line with the mechanistic course previously suggested for related enone [2+2] photocycloaddition reactions,[23,27] in which a triplet 1,4-diradical state (T-DR) is proposed to be the key intermediate of the reaction. Adapted to the reaction of quinolones, a picture evolves as drawn in Scheme 7 for the proto-

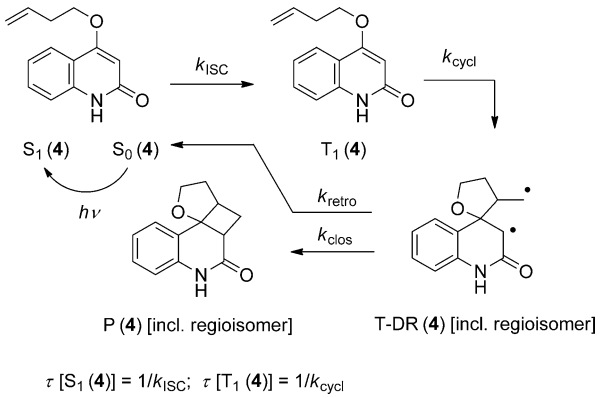

Scheme 7. Mechanistic scheme for the intramolecular [2+2] photocycloaddition of substrate **4** serving as a general scheme for the discussion of all other quinolone substrates (for nomenclature and abbreviations, see narrative). For the structure of the crossed regioisomer, see Scheme 1.

typical substrate **4**. The triplet 1,4-diradical is formed from the T_1 state, which in turn is populated from the respective singlet excited state with the ISC rate constant k_{ISC}. For all substrates **4**, **6**–**9**, which can undergo an intramolecular [2+2] photocycloaddition, the triplet state lifetime τ [T_1] is limited by the cyclization to the triplet 1,4-diradical T-DR. The cyclization occurs between the photoactivated double bond and the adjacent carbon–carbon double bond of the side chain, which is not part of the absorbing chromophore. In agreement with previously reported rate constants for k_{cycl} in enone [2+2] photocycloaddition reactions[28] this process is rapid and occurs on the timescale of τ [T_1] $\approx$ 1 ns (Table 1).

The observed lifetimes τ [T-DR], which fit very well to previously reported triplet 1,4-diradical lifetimes,[29] strongly support the assignment of the spectral signatures of the occurring intermediates to the respective triplet 1,4-diradicals. Although the determined reaction kinetics suggest a close to unity quantum yield for the population of the triplet 1,4-diradical state, the actinometrically determined quantum yields Φ_P for product formation are clearly below unity (see Table 1). Therefore branching reaction kinetics, in which one state is depopulated by two competing processes with comparable probabilities, can be assumed. The ring-closure (k_{clos}) and the retrocleavage (k_{retro}) are likely to be responsible for the branching leading to the product in one reaction channel and to the starting material in the other reaction channel. A putative singlet 1,4-diradical (S-DR; not shown in Scheme 7) is spectroscopically inaccessible, since its population rate is presumably much lower than the sum of depopulation rates k_{retro} and k_{clos}. Still, since the lifetime τ [T-DR] of the triplet 1,4-diradical stays constant within the measurement error for both chromophores, the branching between product formation and retrocleavage likely occurs not in the triplet 1,4-diradical state but happens in the singlet 1,4-diradical.

The ratio of k_{clos} and k_{retro} is to some extent influenced by the substitution pattern of the side chain. The *cis* configuration of the ethyl group in (*Z*)-**6** for instance favors the second bond formation (Table 1) leading to a higher product quantum yield Φ_P for (*Z*)-**6** (0.72) than for (*E*)-**6** (0.32). The higher quantum yield is qualitatively reflected by the previously mentioned higher conversion of (*Z*)-**6** (60%) as compared with (*E*)-**6** (44%) after five minutes of irradiation. A terminal dimethyl substitution favors the retrocleavage over the ring-closure as evident when comparing these substrates to the respective unsubstituted alkenyloxyquinolones (cf., **4** vs. **7** and **8** vs. **9** in Table 1).

Based on a sequential rate model, taking the determined rates, spectra, and states into account, the species-associated absorption spectra (SAS) of the T_1 and the triplet 1,4-diradical state can be extracted from the transient data matrices. The obtained spectrum for the T_1 state of **4** is in agreement with the previously published T_1 absorption spectra of related compounds[7a,b,8] and shown in Figure 5. The maximum of

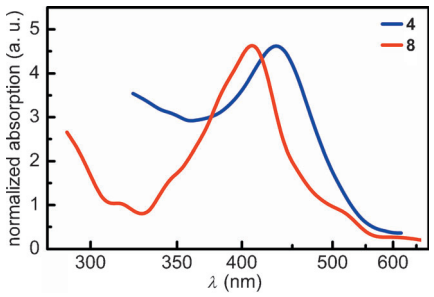

Figure 5. Species-associated absorption spectra (SAS) of the T_1 state of the representative quinolones 4-(but-3-enyl)oxyquinolone (**4**) and 3-(but-3-enyl)oxyquinolone (**8**) after 270 nm excitation in MeCN.

the T–T absorption is observed at $\lambda \approx 450$ nm for **4**, whereas the T–T absorption of the 3-substitued quinolone **8** is blue-shifted to $\lambda \approx 400$ nm.

The calculated SAS of the triplet 1,4-diradical state of both chromophores exhibit a strong, characteristic absorption band centered at around 300 nm (**4**, (*Z*)-**6**, (*E*)-**6**, **7**) and at approximately 350 nm (**8**, **9**) as shown for the 1,4-diradicals derived from **7** and **9** in Figure 6. Interestingly, the triplet 1,4-diradicals of **4**, (*Z*)-**6**, (*E*)-**6** and **7** show an additional, less-intense absorption band centered around 380 nm

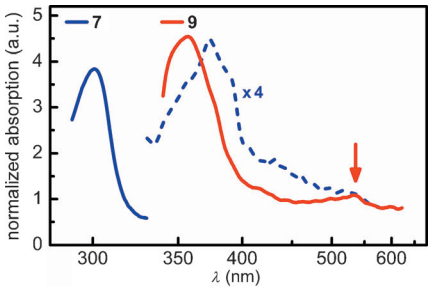

Figure 6. Species-associated absorption spectra (SAS) of the triplet 1,4-diradical (T-DR) states of selected quinolones **7** and **9**.

(dotted blue line, Figure 6), which exhibits a Franck–Condon progression, which is very similar to the $S_1 \leftarrow S_0$ transition (Figure 3a). Also, the triplet 1,4-diradicals derived from compounds **8** and **9** exhibit an additional, redshifted, less-intense absorption band, which could not be well resolved due to a low signal intensity (arrow, Figure 6). Since the spectra of the 1,4-diradical states are well separated from the triplet spectra, transient absorption spectroscopy can be used to differentiate between the two species and follow the course of the [2+2] photocycloaddition reaction.

Enantioselective [2+2] photocycloaddition reactions in the presence of a sensitzer at $\lambda = 366$ nm: Enantioselective reactions were performed in the presence of the chiral sensitizer (+)-**1** or its enantiomer (−)-**1**. The sensitizer is complexed to the substrate with a high association constant and serves two purposes.[16] First, it provides enantioselectivity due to steric hindrance (see below). Second, it ensures at the chosen wavelength a selective excitation only within the substrate-sensitizer complex. The excitation of uncomplexed sensitizer leads to a loss of photons as diffusional activation is kept low by the choice of concentrations. If optical excitation of the substrate is possible within the chosen wavelength a racemic background reaction must be expected due to the large number of uncomplexed substrate molecules.

The reactions were performed at three different temperatures, that is, −25 °C, 0 °C and ambient temperature (RT) employing 10 mol % of the catalyst. For the reactions of the 4-alkenyloxyquinolones the substrate concentration was consistently 5 mM in trifluorotoluene as the solvent. Since the enantioselective reactions of substrate **4** (Scheme 1) had so far been only performed at −25 °C, the reactions were also conducted at higher temperature. Complete conversion was achieved after a reaction time of 50 min. At 0 °C the yield was 84 % with a regioselectivity of r.r. = 76:24, the major regioisomer **5** showing an enantiomeric excess of 91 %. At ambient temperature the total yield was 82 % with an r.r. of 81:19 and 88 % *ee* for the straight product **5**. In previous work the enantioselectivity for the reaction of substrate **2** (Scheme 1) had been determined to be 11 % *ee* at 30 °C and 15 % *ee* at 0 °C.

Due to the occurrence of three isomers, the [2+2] photocycloaddition of substrates **6** was (among all reactions studied) the most complex to analyze and the results are comprehensively provided in Table 2. The reaction yields were high for either starting diastereoisomer (*E*)-**6** (Table 2, entries 1–3) or (*Z*)-**6** (Table 2, entries 4–6). As observed in the racemic series, the influence of the starting olefin configuration was minimal. The *Z* isomer delivered slightly higher selectivities regarding the formation of regioisomers and diastereoisomers, the effect being most pronounced at room temperature (Table 2, entries 1 and 4). In this category, however, the most remarkable effect is exerted by the catalyst. If compared under otherwise identical conditions to the racemic series (Scheme 4), the r.r. increased from 60:40 to 76:24 (Table 2, entry 1) for (*E*)-**6** and from 65:35 to 86:14 (Table 2, entry 4) for (*Z*)-**6**. The d.r increased from 51:49 to 76:24 (entry 1) for (*E*)-**6** and from 77:23 to 85:15 (entry 4) for (*Z*)-**6**.

Table 2. Enantioselective intramolecular [2+2] photocycloaddition of quinolones **6** at $\lambda = 366$ nm to provide enantiomerically enriched products **14** and **15**.[a]

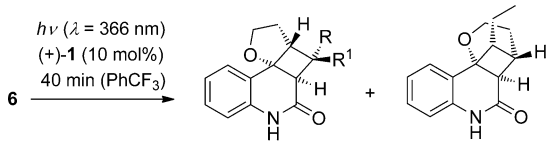

Entry		*T* [°C]	Yield[b] [%]	r.r.[c] **14**:**15**	d.r.[c] **14a**:**14b**	*ee*[d] [%] (**14a**)	*ee* [%] (**14b**)	*ee* [%] (**15**)
1	(*E*)-**6**	RT	93	76/24	76/24	78	72	68
2	(*E*)-**6**	0	89	82/18	82/18	90	82	74
3[e]	(*E*)-**6**	−25	91	82/18	85/15	92	84	74
4	(*Z*)-**6**	RT	91	86/14	85/15	80	70	66
5	(*Z*)-**6**	0	89	88/12	88/12	88	78	68
6[e]	(*Z*)-**6**	−25	90	88/12	88/12	92	84	70

[a] All reactions were conducted at the indicated temperature *T* by using a RPR-100 reactor with sixteen 366 nm, 8 W fluorescent lamps (e.g., Philips black light blue; emission spectrum, see the Supporting Information) as the irradiation source in dry, deaerated trifluorotoluene ($c = 5$ mM) as the solvent. [b] Yield of isolated product. [c] The ratio of regioisomers (r.r.) and diastereoisomers (d.r.) ratio was determined by HPLC. [d] The enantiomeric excess (*ee*) was determined by chiral HPLC after separation of the individual isomers **14a**, **14b**, and **15**. [e] The irradiation time was 45 min.

The enantiomeric excess was measured for the individual products after having completely separated the three isomers **14a**, **14b**, and **15** by preparative HPLC. The absolute configuration was assigned based on analogy to the known configuration of compound **3** and of a crossed product related to **15**. The assignment is supported by specific rotation data.[9] In general, the enantiomeric excesses decreased in the order **14a** > **14b** > **15**. By comparing Table 2 entries 1 versus 4, 2 versus 5, and 3 versus 6 it is obvious that the influence of the starting olefin geometry does not significantly influence the *ee* value. However, there is a temperature influence, which has also been observed for substrate **4**. Lower reaction temperatures favor an enantioselective product formation.

The temperature effect was slightly more pronounced for substrate **7** compared with substrate **4**. The former quino-

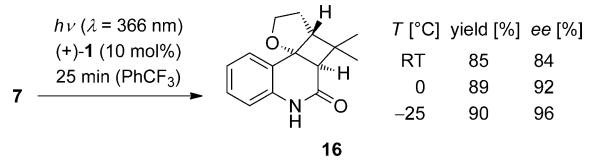

T [°C]	yield [%]	ee [%]
RT	85	84
0	89	92
−25	90	96

Scheme 8. Highly enantioselective intramolecular [2+2] photocycloaddition of 4-(4-methylpent-3-enyl)oxyquinolone (**7**) to product **16**.

lone reacted with excellent, so far unprecedented enantioselectivity at −25 °C (96 % *ee*) and at 0 °C (92 % *ee*) but showed a lower selectivity (84 % *ee*) at room temperature (Scheme 8). Yields of the [2+2] photocycloaddition product **16** were consistently high and the enantioselectivities are remarkable given that only 10 mol % of the catalyst was used (Scheme 8). In particular, the reaction outcome at −25 °C (90 % yield, 96 % *ee*) powerfully demonstrates that enantioselective catalytic photochemistry is getting competive with other areas of enantioselective organocatalysis.

Compared with the high enantioselectivities achieved with 4-alkenyloxyquinolones **4** and **7**, the results obtained with their 3-substituted analogues **8** and **9** were somewhat disappointing. Due to a lower solubility, these reactions were performed at a substrate concentration of $c = 2.5$ mM in trifluorotoluene. The enantiomer (−)-**1** of catalyst (+)-**1** was employed for reasons of supply. Compound **1** is prepared racemically[16] and subsequently separated by chiral HPLC delivering equal amounts of (−)-**1** and (+)-**1**. To keep the nomenclature consistent the major enantiomers obtained from (−)-**1**, which is the enantiomer *ent*-**1** of (+)-**1**, are named *ent*-**17** and *ent*-**18**. The [2+2] photocycloaddition reactions proceeded rapidly and delivered the respective products in high yields of 83–88 %. The enantioselectivity increased with a decrease of the reaction temperature (Table 3; entries 1–3, entries 4–6) but did not exceed 64 % *ee*.

Since enantioselective [2+2] photocycloaddition reactions of 3-substituted quinolones have not yet been studied, it was desirable to prove the absolute configuration of the products, when produced in the presence of a chiral 1,5,7-trimethyl-3-azabicyclo[3.3.1]nonan-2-one. To this end, the minor enantiomer **17** of the reactions discussed above was separated by chiral HPLC and converted into the respective bromo compound **21** (Scheme 9) by treatment with *N*-bromosuccinimide (NBS). The absolute configuration of this product was unambiguously determined by anomalous X-ray diffraction (see the Supporting Information for further details).

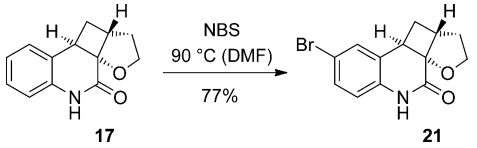

Scheme 9. Preparation of the bromo compound **21**, the absolute configuration of which was elucidated by anomalous X-ray diffraction.

Table 3. Enantioselective intramolecular [2+2] photocycloaddition of quinolones **8** and **9** at $\lambda = 366$ nm to provide enantiomerically enriched products *ent*-**17** and *ent*-**18**, respectively.[a]

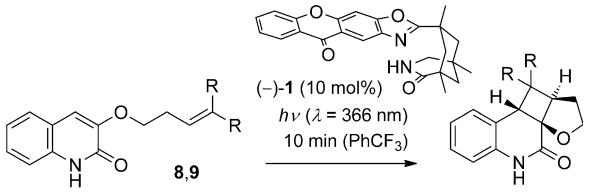

Entry		R	T [°C]	Yield[b] [%]	ee[c] [%]
1	**8**	H	RT	85	46
2	**8**	H	0	83	54
3[d]	**8**	H	−25	85	64
4	**9**	Me	RT	86	58
5	**9**	Me	0	88	60
6	**9**	Me	−25	85	60

[a] All reactions were conducted at the indicated temperature *T* by using a RPR-100 reactor with sixteen 366 nm, 8 W fluorescent lamps (e.g., Philips black light blue; emission spectrum, see the Supporting Information) as the irradiation source in dry, deaerated trifluorotoluene ($c = 2.5$ mM) as the solvent. [b] Yield of isolated product. [c] The enantiomeric excess was determined by chiral HPLC. [d] The irradiation time was 15 min.

Factors governing the stereoselectivity in the [2+2] photocycloaddition reaction: A major outcome of the photophysical studies is the fact that they substantiate the previous assumption of a high cyclization rate k_{cycl} (i.e., a short triplet lifetime) favoring high enantioselectivity. Substrates **4**, **6**, and **7** show triplet state lifetimes in the order of 1 ns, whereas the triplet state lifetime of **2** is much higher. In the latter case the dissociation rate from catalyst (+)-**1** is apparently in the order of the cyclization rate (10^7–10^8 s^{-1}) accounting for a large fraction of reactions to occur after dissociation from the catalyst. The enantioselectivity of the reaction **2**→**3** is consequently low (see above). As shown in Scheme 7, the cyclization step determines the absolute configuration of the product irrespective of its regioselectivity. An enantioface differentiation occurs in a 1,5,7-trimethyl-3-azabicyclo-[3.3.1]nonan-2-one with benzoxazolyl substituents of any kind in position 7 because the substituent shields effectively one face of the quinolone double bond from an attack. The fidelity of this shielding is high even at ambient temperature as clearly seen by the enantioselectivities achieved with substrates **4** (88 % *ee*) and **7** (84 % *ee*) at ambient temperature. The slightly lower enantioselectivitiy in the reactions of 4-(hex-3-enyl)oxyquinolones (**6**→**14a**) (Table 2, entries 1 and 4) could be accounted for by their slightly lower cyclization rate. The decreased enantioselectivity observed for the crossed product **15** is likely due to the slower rate of six-membered ring formation.

The approach of a tethered olefin occurs in quinolones complexed to the enantiomer (−)-**1** of sensitizer (+)-**1** of course from the opposite face explaining the formation of *ent*-**17** and *ent*-**18** in significant enantiomeric excesses (Figure 7). To explain the lower enantioselectivity achieved

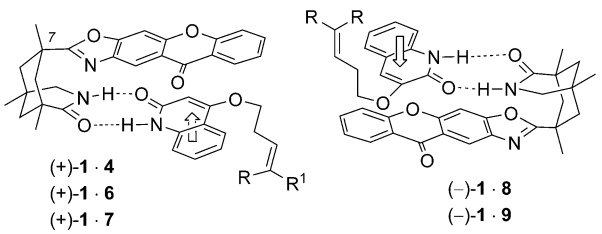

Figure 7. Preferred approach (→) of the tethered olefin in the complexes of (+)-**1** and (−)-**1** with the respective 4-alkenyloxyquinolones **4**, **6**, **7** (left) and 3-alkenyloxyquinolones **8**, **9** (right).

with substrates **8** and **9** (relative to substrates **4**, **6**, and **7**), the absorption properties of these compounds must be taken into account. Both quinolones **8** and **9** show a significantly stronger absorption at $\lambda \approx 350$ nm in the UV/Vis spectrum, which allows for a relatively rapid background reaction under the irradiation conditions. When reactions were performed at room temperature in the absence of sensitizer (−)-**1** under conditions otherwise identical to the conditions of Table 3, yields of 21% (for *rac*-**17**) and 17% (for *rac*-**18**) were obtained after an irradiation time of ten minutes. In other words, the background reactions account for an *ee* loss of at least 20 percentage points.

From the lifetimes for the triplet intermediates T-DR (Scheme 7, Table 1) and the dissociation rate from templates (+)-**1** and (−)-**1** (see above) it is likely that a non-negligible fraction of these intermediates is still bound to the sensitizer before cyclobutane ring formation. This assumption is in agreement with the fact that the sensitizer influences the diastereo- and regioselectivity in the reaction of 4-(hex-3-enyl)oxyquinolones (**6**) (Scheme 4 vs. Table 2). Diastereoisomers (**14b**) and constitutional isomers (**15**), which lead to an increased steric repulsion with the xanthone moiety, are disfavored (Table 2).

Conclusion

In this study a key principle for the design of chiral photocatalysts has been confirmed. The enantioselectivity determining step of the desired reaction must occur fast enough to compete with substrate dissociation from the photocatalyst. For the currently used xanthone **1**, this requirement asks for C−C bond-forming reactions on the ns timescale. As proven by transient absorption spectroscopy, the cyclization of substrates **4**, **6**–**9** does occur within this time window guaranteeing excellent selectivity for the formation of products **5**, **14**, and **16**. If the cyclization is slower, for example, for the formation of product **3** from **2** or of product **15** from **6**, the enantioselectivity decreases.

In addition, it became again evident in this study that the success of the enantioselective catalysis depends on an appropriate choice of excitation wavelength and on the absorption properties of the substrate and the respective substrate–photocatalyst complex. If excitation can occur in the absence of the photocatalyst, background reactions lead to a deterioration of enantioselectivity, as observed for substrates **8** and **9**.

The transient absorption spectroscopy results not only corroborate this analysis but they also provide valuable data for further investigations. Although the enantioselective process within the substrate complexes depicted in Figure 7 appears understood, it is not yet clear how the energy transfer within this complex is accomplished on a molecular level. Operationally more difficult studies are required to investigate the substrate–photocatalyst complex by transient absorption spectroscopy. The data and spectra now obtained (Figures 4–6) present an excellent starting point for further work. Dexter energy transfer[30] is certainly conceivable and has been previously discussed[9,16] but requires to be proven in the context of further experiments. Work along these lines is ongoing in our laboratories.

Experimental Section

General: All reactions sensitive to air or moisture, were carried out in flame-dried glassware under argon pressure using standard Schlenk techniques. Photochemical experiments were performed in flame-dried pyrex irradiation tubes (diameter: 1.0 cm, volume: 15 mL for low-temperature irradiation) under argon pressure. Irradiation experiments were performed in a Rayonet RPR-100 photochemical reactor (Southern New England Ultra Violet Company, Branford, CT, USA) equipped with fluorescence lamps (Philips black light blue 8 W, $\lambda_{max} = 366$ nm; Rayonet RPR-3000 Å, $\lambda_{max} = 300$ nm). For the photochemical reactions dry α,α,α-trifluorotoluene was used and degassed by purging with argon in an ultrasonicating bath for 15 min. Flash chromatography was performed on silica gel 60 (Merck, 230–400 mesh) with the eluent mixtures given in the corresponding procedures. Thin layer chromatography (TLC) was performed on silica-coated glass plates (silca gel 60 F 254). Compounds were detected by UV ($\lambda = 254$ nm, 366 nm) fluorescence. All solvents for chromatography were distilled prior to use. Preparative HPLC separations were performed on a Waters HPLC system (flow rate: 20 mL min^{-1}; achiral stationary phase: XBridge C18 column, 5 μm, 30×150 mm; eluent: H_2O/MeCN = 70:30, 1% trifluoroacetic acid) with a flame ionization detector. The temperature method is given for the corresponding compounds. Analytical HPLC was performed using a chiral stationary phase (Daicel ChiralCell, Chemical Industries, flow rate: 1.0 mL min^{-1}, type and eluent are given for the corresponding compounds) and UV detection. IR: JASCO IR-4100. MS/HRMS: Thermo Scientific DFS HRMS. ^{1}H and ^{13}C NMR: Bruker AV-360 and AV-500 recorded at 300 K. Chemical shifts are reported relative to the solvent [$CHCl_3$: $\delta(^1H) = 7.26$ ppm, $\delta(^{13}C) = 77.0$ ppm, [D_5]DMSO: $\delta(^1H) = 2.50$ ppm, $\delta(^{13}C) = 39.5$ ppm] as reference. Apparent multiplets that occur as a result of accidental equality of coupling constants to those of magnetically non-equivalent protons are marked as virtual (virt.). The relative configuration of chiral products and the multiplicity of the ^{13}C NMR signals were determined by two-dimensional NMR spectra (COSY, NOESY, HSQC, HMBC). Specific rotations were determined by using a PerkinElmer 241 MC polarimeter (sodium vapor lamp). Melting points were measured on a Büchi 510 of the company Büchi and are not corrected.

Transient absorption spectroscopy on multiple timescales: The femtosecond broadband pump-probe setup has been described in detail elsewhere.[31] Briefly, a Ti/sapphire amplifier system (CPA 2001, Clark-MXR) with a repetition rate of 1 kHz was used to pump a noncollinear optical parametric amplifier (NOPA) which provides pulses with a center wavelength of 540–550 nm. After compression and frequency doubling in a BBO-crystal (100 μm thickness) we achieved pump pulses with a center wavelength of 270–275 nm and sub-ps duration. The beam with a pulse energy of about 400 nJ was focused with a spot size of 100–150 μm

(FWHM) into a 1 mm flow cell containing the sample solution with an optical density below 1 within the spectral probe range. A supercontinuum (290–750 nm) was generated and used as probe by focusing another part of the Ti/sapphire laser into a rotating CaF_2 (4 mm thickness) disk. The relative polarization of pump and probe pulses was set to the magic angle (54.7°) to avoid contributions from the rotational relaxation to the observed kinetics. A computer controlled delay line was used to set pump–probe delays up to 2 ns. After the interaction in the sample, the probe light was dispersed with a fused silica prism and detected with a 524 pixel CCD. The chirp of the white light was corrected for prior to data analysis. The resulting temporal resolution was better than 100 fs.

For transient absorption measurements on the ns timescale we used a pulsed ns laser system (NT242, Ekspla) with 1 kHz repetition rate and integrated OPO for spectral tunability, to pump the sample in a 1 mm flow cell (see above). The ns laser is externally triggered and is electronically synchronized with the Ti/sapphire amplifier system (see above), running at 1 kHz repetition rate as well. We still use the supercontinuum, generated by focusing the fs pulses into a CaF_2 disk for probing the sample. The pump–probe delay Δt is set by a computer controlled delay generator, which introduces a specified temporal delay Δt in the electronic trigger pulse from the master oscillator before the pulse triggers the release of the ns excitation pulse. This setup for transient absorption spectroscopy, combining two electronically connected laser sources, provides a temporal resolution better than 2.5 ns and allows recording transient absorption spectra up to temporal delays in the 100 μs regime.

To obtain kinetics from the TA data we used a global data analysis that is based on a formalism developed by Fita et al.[32] and extracts decay associated difference spectra (DADS) from the transient data.[31] Before applying the global fit routine to our TA data, the wavelength scale was rescaled to a scale linear in ΔE to avoid he enhancement of the weight of the long-wave components. The global fit analysis provides a global set of time constants τ_i and the corresponding DADS $A_i(\lambda)$.

$$\Delta OD(\lambda, t) = \sum_i A_i(\lambda) \exp\left(-t/\tau_i\right) \quad (1)$$

Further data processing and the calculation of the species associated absorption spectra (SAS) were based on inserting the obtained DADS $A_i(\lambda)$ into a sequential rate model.

Actinometric measurements: We used the previously mentioned ns laser system with integrated OPO, which provides a spatially, spectrally and energetically well-defined light beam, for photo-excitation of the sample solution in a transparent cuvette. A very similar approach, but using LEDs as light source for the determination of product quantum yields has been reported.[33] The irradiation was performed in a standard 10 mm cuvette containing about 3.8 mL sample solution, exhibiting an optical density of about 1.2 at the absorption maximum at 317 nm while stirring with a magnetic stirring bar. This ensures that more than 90% of the incident photons at $\lambda = 317$ nm are absorbed. We measured P_{trans}, the light intensity transmitted by the sample solution, and P_{ref}, the light intensity transmitted by a reference solution comprising just solvent in a similar cuvette.

$$N_{abs} = \frac{(P_{ref} - P_{trans})\Delta t}{E_\gamma} \quad (2)$$

The decrease in absorption intensity of the starting material at 317 nm was used for the calculation of the amount of converted starting material within the irradiation time. In each case, we measured 3 data points for an over-all conversion of typically below 20% of the total amount of sample in the cuvette. The quantum yield then was the ratio of formed product molecules N_{prod} and absorbed photons N_{abs}.

Representative procedure for the [2+2] photocycloaddition at short wavelength ($\lambda \approx 300$ nm) leading to racemic products: 1,1-dimethyl-1,2,3,10b-tetrahydro-1*H*-furo[2′,3′:1,4]cyclobuta[1,2-c]quinolin-5(6*H*)-one (*rac*-18): Compound **9** (61.0 mg, 0.25 mmol) was dissolved in α,α,α-trifluorotoluene (100 mL, $c = 2.5$ mmol L^{-1}). The solution was irradiated at $\lambda = 300$ nm (light source: RPR-3000 Å, emission spectrum, see the Supporting Information) at ambient temperature for 10 min. The solvent was removed in vacuo and the resulting oil was purified by flash column chromatography (50 g silica, pentane/EtOAc = 2:1). The racemic compound *rac*-**18** was obtained as a colorless solid (57.7 mg, 0.24 mmol, 95%). R_f = 0.62 (EtOAc [UV]); m.p. = 158–160 °C; ^{1}H NMR (500 MHz, $CDCl_3$, 303 K, TMS): $\delta = 8.15$ (br s, 1H; NH), 7.15 (virt. td, $^3J \approx 7.8$ Hz, $^4J =$ 1.3 Hz, 1H; H-8), 6.98 (virt. td, $^3J \approx 7.6$ Hz, $^4J = 1.1$ Hz, 1H; H-9), 6.90 (dd, $^3J = 7.5$ Hz, $^4J = 1.3$ Hz, 1H; H-10), 6.74 (dd, $^3J = 7.9$ Hz, $^4J = 1.1$ Hz, 1H; H-7), 4.45 (ddd, $^2J = 9.0$ Hz, $^3J = 7.7$ Hz, $^3J = 3.1$ Hz, 1H; H-3α), 4.15 (*virt*.td, $^2J \approx {}^3J = 9.3$ Hz, $^3J = 6.5$ Hz, 1H; H-3β), 3.29 (s, 1H; H-10b), 2.94 (virt. dt, $^3J = 8.9$ Hz, $^3J \approx {}^4J = 1.8$ Hz, 1H; H-1a), 2.27–1.90 (m, 2H; H-2), 1.16 (s, 3H; CH_3), 0.81 ppm (s, 3H; CH_3); ^{13}C NMR (250 MHz, $CDCl_3$, 303 K, TMS): $\delta = 170.4$ (s, C-5), 136.5 (s, C-6a), 128.5 (d, C-10), 127.8 (d, C-8), 123.5 (d, C-9), 121.6 (s, C-10a), 115.8 (d, C-7), 78.3 (s, C-4), 71.0 (t, C-3), 56.6 (d, C-1a), 50.5 (d, C-10b), 34.9 (s, C-1), 27.8 (t, C-2), 26.4 (q, CH_3), 24.8 ppm (q, CH_3); IR (ATR): $\tilde{\nu} = 2942$, 2356, 1682, 1594, 1495, 1389, 1143, 1076, 1048, 973, 827 cm^{-1}; MS (EI, 70 eV): m/z (%) = 243 (1) [M^+], 212 (1), 198 (2), 174 (3) [$M^+ - C_5H_9$], 161 (100) [$M^+ - C_6H_{10}$], 143 (5) [$M^+ - C_6H_{12}O$], 133 (3) [$M^+ - C_7H_{10}O$], 115 (5), 104 (3) [$M^+ - C_8H_{11}O_2$], 89 (4) [$C_7H_5^+$], 83 (7), 77 (3) [$C_6H_5^+$], 67 (2), 55 (15); HRMS (EI): m/z: calcd for $C_{15}H_{17}O_2N$: 243.1254; found: 243.1254.

Representative procedure for the enantioselective [2+2] photocycloaddition under sensitized conditions at $\lambda \approx 366$ nm: (3a*S*,4a*S*,10b*S*)-4,4-dimethyl-2,3,4,4a-tetrahydro-furo-[2′,3′:2,3]-cyclobuta[1,2-c]-quinolin-5-(6*H*)-one (16): Compound **7** (12.2 mg, 50.0 μmol) and (+)-**1** (2.08 mg, 5.00 μmol, 10 mol%) were dissolved in α,α,α-trifluorotoluene (10 mL, $c = 5$ mmol L^{-1}), cooled to −25 °C and irradiated at $\lambda = 366$ nm (light source: Philips black light blue; emission spectrum, see the Supporting Information) for 20 min. Silica (500 mg → dry load) was added and the solvent was evaporated under reduced pressure. Following flash column chromatography (5 g silica, pentane/EtOAc = 1:1), photoproduct **16** was obtained as a colorless solid (11.0 mg, 45.2 μmol, 90%, 96% *ee*). $R_f = 0.64$ (EtOAc [UV]); HPLC (chiral phase AD-H, *n*-hexane/*i*PrOH = 90:10, 1 mL min^{-1}, $\lambda = 210$ and 254 nm): $t_R = 12.6$ min [*ent*-**16**], 13.6 min [**16**]; m.p. = 122–126 °C; $[\alpha]_D^{20} = +11.2$ ($c = 0.9$, MeOH) [96% *ee*]; ^{1}H NMR (500 MHz, $CDCl_3$, 303 K, TMS): $\delta = 8.35$ (brs, 1H; NH), 7.30 (d, $^3J =$ 7.7 Hz, 1H; H-10), 7.21 (virt. t, $^3J \approx 7.7$ Hz, 1H; H-8), 7.05 (virt. t, $^3J \approx 7.5$ Hz, 1H; H-9), 6.73 (d, $^3J = 8.0$ Hz, 1H; H-7), 4.42–4.34 (m, 1H; H-2α), 4.09–3.99 (m, 1H; H-2β), 3.02 (s, 1H; H-4a), 2.57 (d, $^3J = 9.2$ Hz, 1H; H-3a), 2.10–2.04 (m, 2H; H-3), 1.21 (s, 3H; CH_3), 1.12 ppm (s, 3H; CH_3); ^{13}C NMR (126 MHz, $CDCl_3$, 303 K, TMS): $\delta = 168.5$ (s, C-5), 136.3 (s, C-6a), 129.5 (d, C-8), 127.7 (d, C-10), 124.2 (d, C-9), 124.0 (s, C-10a), 115.5 (d, C-7), 79.4 (s, C-10b), 68.9 (t, C-2), 58.1 (d, C-3a), 51.8 (d, C-4a), 34.8 (s, C-4), 27.8 (t, C-3), 26.1 (q, CH_3), 24.8 ppm (q, CH_3); IR (ATR): $\tilde{\nu} = 2925$ (w, ArH), 2861 (w, $C_{al}H$), 1662 (s, C=O), 1594 (m, NH), 1381 (s), 1274 (s), 1139 (s), 1063 (s), 1039 cm^{-1} (vs, C-O); MS (EI, 70 eV): m/z (%): 243 (70) [M^+], 161 (100) [$M^+ - C_6H_{10}$], 82 (40), 67 (23), 55 (69), 44 (44); HRMS (EI): m/z: calcd for $C_{15}H_{17}NO_2$: 243.1254; found: 243.1254.

Single-crystal X-ray absolute structure determination of compound 21: Formula: $C_{13}H_{12}BrNO_2$; $M_r = 294.14$; crystal color and shape: pale-yellow fragment, crystal dimensions = 0.15 × 0.15 × 0.20 mm; crystal system: triclinic; space group $P1$ (no. 1); $a = 6.4063(3)$, $b = 9.8661(5)$, $c =$ 10.3432(5) Å; $\alpha = 114.362(2)$, $\beta = 103.133(2)$, $\gamma = 95.359(2)°$, $V =$ 566.91(5) Å^3; $Z = 2$; $\mu(Mo_{K\alpha}) = 3.613$ mm^{-1}; $\rho_{calcd} = 1.723$ g cm^{-3}; $F_{000} =$ 296; $T = 123$ K; θ range = 2.3–25.4°; data collected: 18004; independent data [$I_o > 2\sigma(I_o)$/all data/R_{int}]: 3951/3951/0.048; data/restraints/parameters: 3951/0/307; $R1$ [$I_o > 2\sigma(I_o)$/all data]: 0.0244/0.0247; $wR2$ [$I_o > 2\sigma(I_o)$/all data]: 0.0658/0.0663; GOF = 1.098; $\Delta\rho_{max/min}$: 0.448/−0.329 e Å^{-3}. Flack parameter $x = 0.045(7)$. Hooft parameter $y = 0.092(6)$. For more details see the Supporting Information. CCDC-919729 (**21**) contains the supplementary crystallographic data for this paper. These data can be obtained free of charge from The Cambridge Crystallographic Data Centre via www.ccdc.cam.ac.uk/data_request/cif.

Acknowledgements

This project was supported by the Deutsche Forschungsgemeinschaft (DFG) in the framework of the DFG Research Training Group "Chemical Photocatalysis" (GRK 1626). M.M.M. and M.W. acknowledge fellowship support by the GRK. R.A. is the recipient of an Alexander von Humboldt research fellowship. We thank Olaf Ackermann and Georg Rudolf (AK Sieber) for help with the HPLC analysis.

[1] General reviews on [2+2] photocycloaddition reactions: a) J. P. Hehn, C. Müller, T. Bach in *Handbook of Synthetic Photochemistry* (Eds.: A. Albini, M. Fagnoni), Wiley-VCH, Weinheim, **2009**, pp. 171–215; b) S. A. Fleming in *Molecular and Supramolecular Photochemistry, Vol. 12* (Eds.: A. G. Griesbeck, J. Mattay), Marcel Dekker, New York, **2005**, pp. 141–160; c) P. Margaretha in *Molecular and Supramolecular Photochemistry, Vol. 12* (Eds.: A. G. Griesbeck, J. Mattay), Marcel Dekker, New York, **2005**, pp. 211–237; d) J. P. Pete in *CRC Handbook of Organic Photochemistry and Photobiology*, 2nd ed. (Eds.: W. Horspool, F. Lenci), CRC, Boca Raton, **2004**, pp. 71/1–71/14; e) T. Bach, *Synthesis* **1998**, 683–703; f) J.-P. Pete, *Adv. Photochem.* **1996**, *21*, 135–216; g) J. Mattay, R. Conrads, R. Hoffmann in *Methoden der Organischen Chemie (Houben-Weyl), Vol. E21c*, 4th ed. (Eds.: G. Helmchen, R. W. Hoffmann, J. Mulzer, E. Schaumann), Thieme, Stuttgart **1995**, pp. 3085–3132; h) M. T. Crimmins, T. L. Reinhold, *Org. React.* **1993**, *44*, 297–588.

[2] a) G. R. Evanega, D. L. Fabiny, *Tetrahedron Lett.* **1968**, *9*, 2241–2246; b) G. R. Evanega, D. L. Fabiny, *J. Org. Chem.* **1970**, *35*, 1757–1761; c) G. R. Evanega, D. L. Fabiny, *Tetrahedron Lett.* **1971**, *12*, 1749–1752.

[3] a) E. C. Taylor, W. W. Paudler, *Tetrahedron Lett.* **1960**, *1*, 1–3; b) I. W. Elliott, *J. Org. Chem.* **1964**, *29*, 305–307; c) O Buchardt, *Acta Chem. Scand.* **1964**, *18*, 1389–1396.

[4] a) B. Loev, M. M. Goodman, K. M. Snader, *Tetrahedron Lett.* **1968**, *9*, 5401–5404; b) T. S. Cantrell, *J. Org. Chem.* **1974**, *39*, 3063–3070; c) R. G. Hunt, C. J. Potter, S. T. Reid, M. L. Roantree, *Tetrahedron Lett.* **1975**, *16*, 2327–2330; d) O. Buchardt, J. J. Christensen, N. Harrit, *Acta Chem. Scand. B* **1976**, *30*, 189–192; e) D. J. Haywood, S. T. Reid, *J. Chem. Soc. Perkin Trans. 1* **1977**, 2457–2458; f) C. Kaneko, T. Naito, M. Somei, *J. Chem. Soc. Chem. Commun.* **1979**, 804–805; g) C. Kaneko, T. Naito, *Chem. Pharm. Bull.* **1979**, *27*, 2254–2256; h) T. Naito, C. Kaneko, *Chem. Pharm. Bull.* **1980**, *28*, 3150–3152; i) C. Kaneko, T. Naito, N. Nakayama, *Chem. Pharm. Bull.* **1981**, *29*, 593–595; j) T. Chiba, M. Okada, T. Kato, *J. Heterocycl. Chem.* **1982**, *19*, 1521–1525; k) C. Kaneko, T. Naito, Y. Momose, H. Fujii, N. Nakayama, I. Koizumi, *Chem. Pharm. Bull.* **1982**, *30*, 519–525; l) T. Naito, Y. Momose, C. Kaneko, *Chem. Pharm. Bull.* **1982**, *30*, 1531–1534; m) C. Kaneko, T. Naito, Y. Momose, N. Shimomura, T. Ohashi, M. Somei, *Chem. Pharm. Bull.* **1983**, *31*, 2168–2171; n) C. Kaneko, N. Shimomura, Y. Momose, T. Naito, *Chem. Lett.* **1983**, 1239–1242; o) T. Naito, C. Kaneko, *Chem. Pharm. Bull.* **1983**, *31*, 366–369; p) T. Chiba, T. Kato, A. Yoshida, R. Moroi, N. Shimomura, Y. Momose, T. Naito, C. Kaneko, *Chem. Pharm. Bull.* **1984**, *32*, 4707–4720; q) S. Nonoyama, N. Yonezawa, K. Saigo, T. Hirano, M. Hasegawa, *Chem. Lett.* **1987**, 487–490; r) M. Sato, K. Kawakami, C. Kaneko, *Chem. Pharm. Bull.* **1987**, *35*, 1319–1321; s) C. Kaneko, T. Suzuki, M. Sato, T. Naito, *Chem. Pharm. Bull.* **1987**, *35*, 112–123; t) S. Nonoyama, N. Yonezawa, K. Saigo, M. Hasegawa, T. Hirano, *Bull. Chem. Soc. Jpn.* **1988**, *61*, 2387–2391; u) E. Sato, Y. Ikeda, Y. Kanaoka, *Liebigs Ann. Chem.* **1989**, 781–788; v) H. Suginome, K. Kobayashi, M. Itoh, S. Seko, A. Furusaki, *J. Org. Chem.* **1990**, *55*, 4933–4943; w) J. Kurita, T. Yamanaka, T. Tsuchiya, *Heterocycles* **1991**, *32*, 2089–2092; x) K. Kobayashi, M. Suzuki, H. Suginome, *J. Org. Chem.* **1992**, *57*, 599–606; y) M. Sakamoto, N. Sato, T. Mino, Y. Kasashima, T. Fujita, *Org. Biomol. Chem.* **2008**, *6*, 848–850; z) F. Yagishita, T. Mino, T. Fujita, M. Sakamoto, *Org. Lett.* **2012**, *14*, 2638–2641.

[5] a) D. F. Cauble, V. Lynch, M. J. Krische, *J. Org. Chem.* **2003**, *68*, 15–21; b) S. Brandes, P. Selig, T. Bach, *Synlett* **2004**, 2588–2590; c) F. Yagishita, M. Sakamoto, T. Mino, T. Fujita, *Org. Lett.* **2011**, *13*, 6168–6171.

[6] Review: J. C. Namyslo, D. E. Kaufmann, *Chem. Rev.* **2003**, *103*, 1485–1537.

[7] a) T. Yamamuro, I. Tanaka, N. Hata, *Bull. Chem. Soc. Jpn.* **1971**, *44*, 667–671; b) T. Yamamuro, N. Hata, I. Tanaka, *Bull. Chem. Soc. Jpn.* **1973**, *46*, 29–34; c) F. D. Lewis, G. D. Reddy, J. E. Elbert, B. E. Tillberg, J. A. Meltzer, M. Kojima, *J. Org. Chem.* **1991**, *56*, 5311–5318.

[8] H. Görner, T. Wolff, *Photochem. Photobiol.* **2008**, *84*, 1224–1230.

[9] C. Müller, M. M. Maturi, A. Bauer, M. C. Cuquerella, M. A. Miranda, T. Bach, *J. Am. Chem. Soc.* **2011**, *133*, 16689–16697.

[10] a) T. Bach, H. Bergmann, K. Harms, *Angew. Chem.* **2000**, *112*, 2391–2393; *Angew. Chem. Int. Ed.* **2000**, *39*, 2302–2304; b) T. Bach, H. Bergmann, *J. Am. Chem. Soc.* **2000**, *122*, 11525–11526; c) T. Bach, H. Bergmann, B. Grosch, K. Harms, *J. Am. Chem. Soc.* **2002**, *124*, 7982–7990; d) S. Breitenlechner, T. Bach, *Angew. Chem.* **2008**, *120*, 8075–8077; *Angew. Chem. Int. Ed.* **2008**, *47*, 7957–7959.

[11] Reviews: a) J. Svoboda, B. König, *Chem. Rev.* **2006**, *106*, 5413–5430; b) D. M. Bassani in *Supramolecular Photochemistry* (Eds.: V. Ramamurthy, Y. Inoue), Wiley, Hoboken, **2011**, pp. 53–86.

[12] T. Bach, H. Bergmann, B. Grosch, K. Harms, E. Herdtweck, *Synthesis* **2001**, 1395–1405.

[13] D. S. Kemp, K. S. Petrakis, *J. Org. Chem.* **1981**, *46*, 5140–5143.

[14] a) P. Selig, T. Bach, *Angew. Chem.* **2008**, *120*, 5160–5162; *Angew. Chem. Int. Ed.* **2008**, *47*, 5082–5084; b) P. Selig, E. Herdtweck, T. Bach, *Chem. Eur. J.* **2009**, *15*, 3509–3525.

[15] Reviews: a) C. Müller, T. Bach, *Aust. J. Chem.* **2008**, *61*, 557–564; b) C. Yang, Y. Inoue in *Supramolecular Photochemistry* (Eds.: V. Ramamurthy, Y. Inoue), Wiley, Hoboken, **2011**, pp. 115–153.

[16] C. Müller, A. Bauer, T. Bach, *Angew. Chem.* **2009**, *121*, 6767–6769; *Angew. Chem. Int. Ed.* **2009**, *48*, 6640–6642.

[17] E. Ochiai, *J. Org. Chem.* **1953**, *18*, 534–551.

[18] a) O. Buchardt, *Acta Chem. Scand.* **1963**, *17*, 1461–1462; b) A. Albini, E. Fasani, L. M. Dacrema, *J. Chem. Soc. Perkin Trans. 1* **1980**, 2738–2742; c) A. Albini, M. Alpegiani, *Chem. Rev.* **1984**, *84*, 43–71.

[19] A. Bakowski, M. Dressel, A. Bauer, T. Bach, *Org. Biomol. Chem.* **2011**, *9*, 3516–3529.

[20] F. Marsais, A. Godard, G. Queguiner, *J. Heterocycl. Chem.* **1989**, *26*, 1589–1594.

[21] T. Nishi, F. Tabusa, T. Tanaka, H. Ueda, T. Shimizu, T. Kanbe, Y. Kimura, K. Nakagawa, *Chem. Pharm. Bull.* **1983**, *31*, 852–860.

[22] a) D. Becker, M. Nagler, S. Hirsh, J. Ramun, *J. Chem. Soc. Chem. Commun.* **1983**, 371–373; b) D. Becker, M. Nagler, Y. Sahali, N. Haddad, *J. Org. Chem.* **1991**, *56*, 4537–4543; c) D. Becker, N. KIimovich, *Tetrahedron Lett.* **1994**, *35*, 261–264.

[23] Review on the mechanism of the [2+2] photocycloaddition, see: D. I. Schuster, G. Lem, N. A. Kaprinidis, *Chem. Rev.* **1993**, *93*, 3–22.

[24] C. Franco, J. Olmsted III, *Talanta* **1990**, *37*, 905–909.

[25] Based on previous work (e.g., A. A. Abdel-Shafi, F. Wilkinson, *J. Phys. Chem. A* **2000**, *104*, 5747–5757), a bimolecular rate constant for triplet state quenching by oxygen can be estimated as $k_q \approx 3 \times 10^9\,\text{M}^{-1}\text{s}^{-1}$. The minimum lifetime of a triplet species in air-equilibrated acetonitrile is consequently $\tau_{min} \geq 1/[k_q \times 2.4\,\text{mM}] \approx 1.3 \times 10^{-7}$ s. Oxygen quenching should not significantly influence the lifetime of a species with an intrinsically shorter lifetime than τ_{min}. Indeed, as seen from Table 1, all intermediates relevant for the [2+2] photocycloaddition processes show lifetimes below 30 ns (3×10^{-8} s).

[26] S. J. Strickler, R. A. Berg, *J. Chem. Phys.* **1962**, *37*, 814–822.

[27] For recent theoretical studies on intramolecular and intermolecular [2+2] photocycloaddition reactions, see: a) S. A. Bradley, B. J. Bresnan, S. M. Draper, N. W. A. Geraghty, M. Jeffares, T. McCabe, T. B. H. McMurry, J. E. O'Brien, *Org. Biomol. Chem.* **2011**, *9*, 2959–2968; b) J. R. Cucarull-González, J. Hernando, R. Alibés, M. Figueredo, J. Font, L. Rodríguez-Santiago, M. Sodupe, *J. Org. Chem.* **2010**, *75*, 4392–4401; c) K. Somekawa, Y. Oda, T. Shimo, *Bull. Chem. Soc. Jpn.* **2009**, *82*, 1447–1469; d) P. Jaque, A. Toro-Labbé, P. Geerlings, F. De Proft, *J. Phys. Chem. A* **2009**, *113*, 332–344.

[28] a) G. Jones II, B. R. Ramachandran, *J. Photochem.* **1976**, *5*, 341–344; b) R. Gleiter, E. Fischer, *Chem. Ber.* **1992**, *125*, 1899–1911; c) D. Becker, Y. Cohen-Arazi, *J. Am. Chem. Soc.* **1996**, *118*, 8278–8284.

[29] a) R. D. Small, J. C. Scaiano, *J. Phys. Chem.* **1977**, *81*, 2126–2131; b) J. C. Scaiano, *Tetrahedron* **1982**, *38*, 819–824; c) D. Becker, N. Haddad, Y. Sahali, *Tetrahedron Lett.* **1989**, *30*, 2661–2664; d) A. Rudolph, A. C. Weedon, *Can. J. Chem.* **1990**, *68*, 1590–1597; e) N. A. Kaprinidis, G. Lem, S. H. Courtney, D. I. Schuster, *J. Am. Chem. Soc.* **1993**, *115*, 3324–3325; f) D. Andrew, D. J. Hastings, A. C. Weedon, *J. Am. Chem. Soc.* **1994**, *116*, 10870–10882; g) J. F. D. Kelly, J. M. Kelly, T. B. H. McMurry, *J. Chem. Soc. Perkin Trans. 2* **1999**, 1933–1941; h) A. D. Cohen, B. M. Showalter, D. A. Brady, C. A. Kenesky, J. P. Toscano, *Phys. Chem. Chem. Phys.* **2003**, *5*, 1059–1063; i) X. Cai, P. Cygon, B. Goldfuss, A. G. Griesbeck, H. Heckroth, M. Fujitsuka, T. Majima, *Chem. Eur. J.* **2006**, *12*, 4662–4667.

[30] D. L. Dexter, *J. Chem. Phys.* **1953**, *21*, 836–850.

[31] U. Megerle, I. Pugliesi, C. Schriever, C. F. Sailer, E. Riedle, *Appl. Phys. B* **2009**, *96*, 215–231.

[32] P. Fita, E. Luzina, T. Dziembowska, C. Radzewicz, A. A. Grabowska, *J. Chem. Phys.* **2006**, *125*, 184508.

[33] U. Megerle, R. Lechner, B. König, E. Riedle, *Photochem. Photobiol. Sci.* **2010**, *9*, 1400–1406.

Received: February 27, 2013
Published online: April 10, 2013

